Temporal variability of spectral Granger causality from neural networks (EEGs) during sleep : a time-frequency approach

Louis Almairac [1] Alexandre André [1] Matthieu Pascal [1] Alexandre Guillet [2] Françoise Argoul [3] Pierre Argoul [4]

[1] École Nationale des Ponts et Chaussées, Département IMI [2] Max Planck Institute for the Physics of Complex Systems [3] LOMA, CNRS UMR5798, Université de Bordeaux [4] LVMT, École Nationale des Ponts et Chaussées, Université Gustave Eiffel

1. Methodological Objective

Develop and validate a time–frequency Granger causality framework based on wavelets to model multivariate interactions in non-stationary time series.

Key Questions :

How to integrate Granger causality locally in both time and frequency ?
What temporal/frequency resolution can be achieved with a Morlet CWT (ω_0, number of cycles) ?
Rigorous comparison between temporal (AIC/BIC) and spectral (Geweke) formulations.

2. Data & Preprocessing

Database : ▪ PhysioNet "MGH Sleep Lab 2018" – Full polysomnographies.
▪ One file contains ≈ 4.5 hours of recording, 42M values, with sleep stages scored every 30s.

Channels : ▪ **EEG** : F3, F4, C3, C4, O1, O2 (frontal, central, occipital)
▪ **EOG (E1, left eye), EMG (Chin), ECG (Thorax), Respiration, SaO_2**

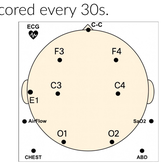

Preprocessing : ▪ **Filtering** : band-pass 0.1–40 Hz ; notch 50 Hz.
▪ **Whitening** : artifact removal outside $[Q_1 - 5\,\mathrm{IQR},\ Q_3 + 5\,\mathrm{IQR}]$.
▪ **Stationarity** : 40s segments validated → tests ADF et KPSS [1]

Frequency bands : ▪ Delta (0.5–4 Hz), Theta (4–8 Hz), Alpha (8–12 Hz), Beta (12–30 Hz), Gamma (30–40 Hz) : .

3. Modeling & Causality

Each 40 s stationary EEG window is modeled by a vector autoregressive process of order $p = 20$ (optimal choice via AIC/BIC). The vector $X_t \in \mathbb{R}^n$ groups the studied signals :

$$X_t = \sum_{k=1}^{p} A_k X_{t-k} + \varepsilon_t$$

This formalism allows for simultaneous modeling of each signal's inherent inertia (auto-regression), cross-influences (inter-channel interactions), and the direction and delay of effects.

Granger Causality (temporal) : Signal j *causes* i if its history reduces the prediction error of i :

$$F_{j\to i} = \ln\left(\frac{\mathrm{Var}(\varepsilon^{i|i})}{\mathrm{Var}(\varepsilon^{i|i,j})}\right), \quad F_{i\cdot j} = \ln\left(\frac{\Sigma_{ii}\Sigma_{jj}}{|\Sigma|}\right)$$

This directional and instantaneous measure is estimated at each window. It is sensitive to order p, noise, and stationarity.

Spectral Causality (frequency) : Geweke's formalism decomposes influence by frequency ω, via the transfer function $H(\omega)$ of the VAR model :

$$f_{j\to i}(\omega) = \ln\left(\frac{S_{ii}(\omega)}{\Sigma_{ii}|H_{ii}(\omega)|^2}\right), \quad f_{i\cdot j}(\omega) = \ln\left(\frac{(\tilde{H}_{ii}(\omega)\Sigma_{jj}\tilde{H}^*_{ii}(\omega))\cdot(\hat{H}_{jj}(\omega)\Sigma_{ii}\hat{H}^*_{jj}(\omega))}{|S(\omega)|}\right)$$

Temporal-Frequency Complementarity : Temporal measures provide an aggregated view, while spectral measures reveal specific bands. The Geweke frequency integral exactly coincides with Granger causality [2, 3, 4] :

$$F_{j\to i} = \frac{1}{2\pi}\int_{-\pi}^{\pi} f_{j\to i}(\omega)\,d\omega, \quad F_{j\cdot i} = \frac{1}{2\pi}\int_{-\pi}^{\pi} f_{j\cdot i(\omega)}\,d\omega$$

Spectro-temporal causality : The spectral density matrix S is defined through Fourier-based method, $S_{lm}(f) = \langle X_l(f)X_m(f)^*\rangle$ and its spectro-temporal expression : $S_{lm}(t,f) = \langle \mathcal{W}_\Psi[X_l](t,f)\,\mathcal{W}_\Psi[X_l](t,f)^*\rangle$.

Wavelet transform of a real signal s : $\mathcal{W}_\Psi[s](b,a) = \langle s, \Psi_{a,b}\rangle = \frac{1}{a^{(1/2)}}\int_{-\infty}^{+\infty} s(t)\Psi^*\left(\frac{t-b}{a}\right)dt,$
with $a = \frac{f_0}{f}$, Ψ the mother wavelet

The spectral density matrix **S** can be factored as : $\mathbf{S}(t,f) = \chi(t,f)\chi^*(t,f)$ [5]
Then the transfer function is retrieved as : $\mathbf{H}(t,f) = \chi(t,f)A_0^{-1}$

Total Causality : The effective causality between two signals combines both directions as well as their instantaneous coupling :

$$F^{\mathrm{tot}}_{i,j} = F_{j\to i} + F_{i\to j} + F_{i\cdot j}$$

It allows estimating the global interaction strength between two sources, independently of the causal direction.

4. Causal Signatures by Phase

For each stable phase (N2, N3, REM), we compute a directional causality matrix between channels, averaged over 50 segments of 30s. Each matrix reveals the functional topology specific to the studied state.

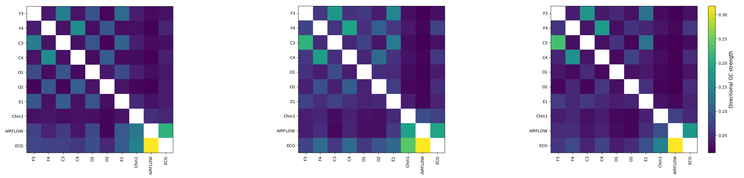

N2 – Light Sleep

Moderate fronto-central coupling (F3/F4 ↔ C3/C4)
Respiratory influence (AIRFLOW, E1 → frontal EEG)
Symmetric bilateral organization

N3 – Deep Sleep

Reinforced F3 ↔ C3 coupling (synchronous slow waves)
Reduction of peripheral influences (EOG, ECG, respiration)
Causality centered on the fronto-central axis

REM – Paradoxical Sleep

Unidirectional frontal causality (F3→ others)
Strong EEG ↔ ECG coupling (cortical–autonomic)
Less symmetry, desynchronized dynamics

5. Spectral Causality (Geweke) – Deep Sleep (N3)

Analysis of average C3 – O2 causality over 50 40-s segments.

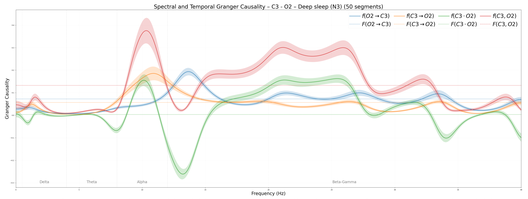

Figure 1 : Average Granger causality between C3 and O2 during deep sleep (N3), estimated over 50 homogeneous windows. Solid curves represent the spectral decomposition of causality. Colored areas indicate 95% confidence intervals. Dotted horizontal lines of the same color represent the average values of the corresponding temporal causality over the analyzed segments.

Observations :

▪ Peak $f_{C3\to O2}$ at 11 Hz (sigma) : antero-posterior spindles.
▪ Inverse peak $f_{O2\to C3}$ at 14 Hz : possible occipito-central return.
▪ < 4Hz : dominant instantaneous causality→delta synchronizatio
▪ > 20Hz : directional causalities decrease, total causality remains significant.

6. Time/Frequency Characterization of EEG Signals

We begin with a spectro-temporal analysis of the C3 channel, typically used in deep sleep, using continuous wavelet transform.

Objective : Visually identify the spectral signatures of different sleep phases.

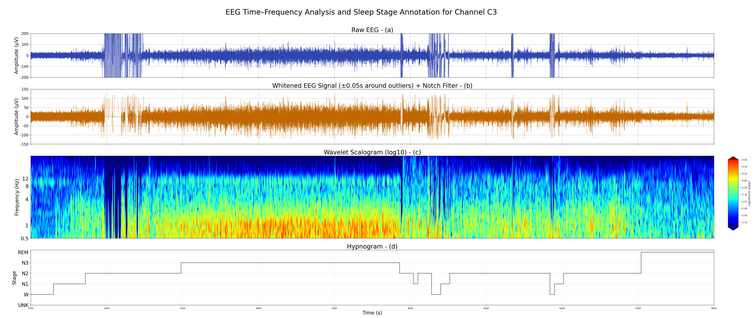

Figure 2 : Multi-scale analysis of the C3–M2 EEG signal during sleep. (a) Raw signal $s(t)$. (b) Artefact-corrected signal $\tilde{s}(t)$ (notch filtering and whitening). (c) Scalogram obtained by Morlet CWT ($\Psi(t) = e^{2i\pi f_0 t}\, e^{\frac{-t^2}{2\sigma^2}}$ where $\sigma = n/2\pi f_0$ with $f_0 = 1$ and $n = 6$), on a logarithmic frequency scale with normalized intensity $\log_{10}(|\mathcal{W}_\Psi[\tilde{s}](t,f)| \,/\, \max_t |\mathcal{W}_\Psi[\tilde{s}](t,f)|)$. (d) Hypnogram. [6].

The multi-scale scalogram (Morlet wavelets, 0.5 ↔ 40 Hz band) reveals cortical synchronization transitions [7] :

- Delta slow waves (< 4 Hz) in N3
- Sporadic Alpha activity (8–12 Hz) in N1/N2
- Faster Beta-Gamma bands more present in REM and Wake

7. Global Study of the C3-O2 Pair

This bidirectional analysis highlights dominant information flows between frontal and occipital regions, revealing the causal signature specific to each sleep stage.

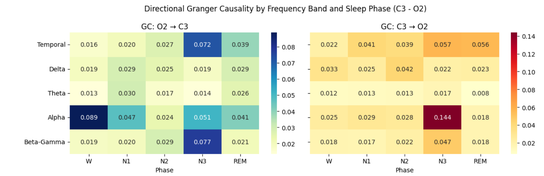

Figure 3 : Directional causalities between C3 and O2 channels, including temporal causality as well as integrated and normalized spectral components in the four frequency bands (Delta, Theta, Alpha, Beta-Gamma), for each of the five sleep phases. The values indicated correspond to averages over 50 segments of the same sleep phase (20 for N1), with a fixed window size (8192 points).

Strong **O2 → C3** flow in N3 (Alpha, Beta-Gamma) : significant occipital influence during deep sleep. **C3 → O2** peak in N3 (Alpha) : possible targeted frontal reactivation or bidirectional coupling. Distinct directional profiles depending on phases → *spectro-temporal dynamics specific to each sleep state.*

8. Time-Frequency Dynamics of Causality

Detailed analysis of Granger causality (Geweke's method) in the time-frequency domain for the information flow 02 → C3.

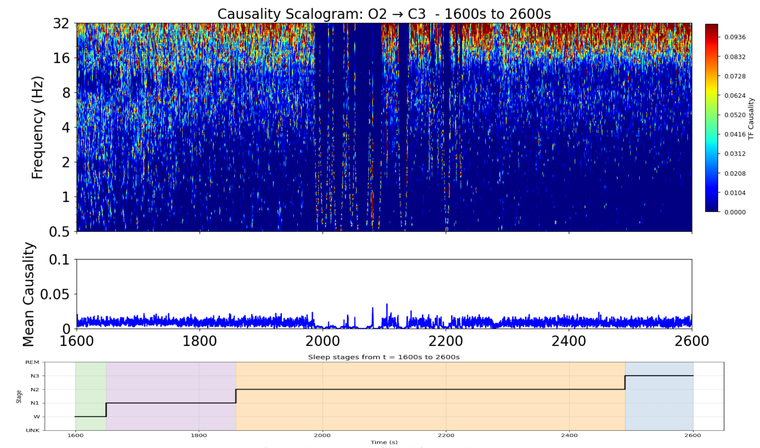

Figure 4 : Causality scalogram (O2 → C3) over a 1000 s window.

Main Observations :

The causal flow is not uniform but concentrates around **specific frequency bands**, with a notable peak in average causality near **30 Hz** (within the Beta range). This causal flow is reinforced in deeper sleep stages.
Causality manifests as **intermittent and transient bursts** rather than continuous flow, indicating dynamic and non-stationary neuronal communication.
The average causality (bottom panel), computed on the whole frequency range presents fluctuations that differ depending on the sleep stage. A further investigation of the nature of these fluctuations in under progress.

9. Conclusions & Methodological Perspectives

Main Contributions :

Introduction of a time–frequency Granger causality metric $f_{j\to i}(t,f)$ via wavelet–Cholesky factorization.
Validation on VAR(3) simulations : precise localization of couplings in [10–40] Hz with ± 0.1 s temporal resolution.
Application to sleep EEG : detection of sigma spindles (11 Hz) and phasic alpha/beta bursts.

Limitations & Future Work :

Optimization of Morlet cycle number and robustness under artefact contamination.
Nonlinear extension : integrate RNNs or kernel methods for strongly non-stationary signals.
Real-time implementation and GPU acceleration for online studies.

10. Main References

[1] A. I. Kaplan, "The problem of the segmental description of the human electroencephalogram," *Human Physiology*, vol. 25, no. 1, pp. 107–114, 1999. Translated from Fiziologiya Cheloveka, 25(1):125–133, 1999.
[2] D. Chicharro, "On the spectral formulation of granger causality," *Biological Cybernetics*, vol. 105, no. 5–6, pp. 331–347, 2011.
[3] M. Ding, Y. Chen, and S. L. Bressler, "Granger causality : Basic theory and application to neuroscience," in *Handbook of Time Series Analysis* (B. Schelter, M. Winterhalder, and J. Timmer, eds.), pp. 437–460, Wiley-VCH, 2006.
[4] A. Shojaie and E. B. Fox, "Granger causality : A review and recent advances," *Annual Review of Statistics and Its Application*, vol. 9, pp. 289–319, 2022.
[5] M. Dhamala, G. Rangarajan, and M. Ding, "Estimating Granger Causality from Fourier and Wavelet Transforms of Time Series Data," *Physical Review Letters*, vol. 100, p. 018701, Jan. 2008.
[6] A. Guillet and F. Argoul, "Uncertainty and information in physiological signals : Explicit physical trade-off with log-normal wavelets," *Journal of the Franklin Institute*, vol. 361, 2024.
[7] H. Huang, K. Yang, Z. Li, Y. Liu, X. Chen, and M. Peng, "Eeg-based sleep staging analysis with functional connectivity," *Sensors*, vol. 21, no. 7, p. 2417, 2021.